



Large-scale shell-model calculations near mass region 100-130

S Dutt^{a*}, Chong Qi^b, Ishtiaq Ahmed^c, I A Rizvi^a & R Kumar^c

^aDepartment of Physics, Aligarh Muslim University, Aligarh 202 002, India

^bRoyal Institute of Technology (KTH), Alba Nova University Center, Stockholm SE 10691, Sweden

^cNuclear Physics Group, Inter-University Accelerator Center, New Delhi 110 067, India

Received 17 February 2020

In this work, we have presented a microscopic shell-model description of the structure and collective behavior of intermediate-mass nuclei around doubly magic ^{100}Sn and ^{132}Sn nuclei. The Sn-isotopes lie between the two doubly magic nuclei and cover a range from exotic proton-rich $N=Z$ nuclei to exotic neutron-rich nuclei with $N/Z > 1.6$. The results obtained using BIGSTICK code for the low-level excitation states and transition probabilities for the studied Sn and Ba isotopic chains have been discussed in the radiance of available experimental data. We have used ^{100}Sn as a core for all the studied isotopes with the same valence space (i.e. $1d_{5/2}$, $2s_{1/2}$, $1d_{3/2}$, $0g_{7/2}$, $0h_{11/2}$ or 'sdgh') for both protons (Z) and neutrons (N) between 50 and 82. These calculations are performed by means of globally optimized monopole effective interaction for the sdgh-shell.

Keywords: Configuration-interaction, Shell-model, BIGSTICK, Transition probability, Excitation energy

1 Introduction

The properties of low-lying states of nuclei in the vicinity of closed shells are important pillars in the understanding of nuclear structure. The variation of nuclear structure with the changing valence nucleons offers an ideal laboratory to understand the developments of nuclear many-body systems and test recent descriptions of single-particle energies (SPE) and residual interactions between valence nucleons. During the last decade, both qualitative and quantitative advancement in shell-model studies has resulted in remarkable achievements in better understanding of nuclear structure^{1,2}. The advancement in the present-day computing facilities has enabled us to take these calculations beyond the mass 100 region with the basis dimension size up to 2×10^{10} . The nuclear shell-model is a full configuration interaction approach. The mixing effects of all possible configurations within a given model space are considered to determine the physical observables defining nuclear properties. For very large dimensions, beyond the present-day limitations, some approximations (truncation) can be made. For no-core shell-model approaches with full configuration interaction, the connection of the effective interaction to fundamental forces and the complexity of their

wave functions are the main challenges in addition to the matrices dimension. In order to overcome the dimensionality limitations many new approximation methods viz. Lanczos method etc. have been developed³⁻⁵. It is also worth to mention here that the nuclear shell-model is by far the most accurate and precise theory available in the market^{1,2}.

The effective interaction used in the present work for the gdsh_{11/2} shell was globally optimized by Chong Qi and Z.X. Xu⁶⁻⁸. They started from the realistic CD-Bonn nucleon-nucleon potential and determined the unknown single-particle energies of the $1d_{3/2}$, $2s_{1/2}$, and $0h_{11/2}$ orbitals and the $T=0,1$ monopole interactions by fitting to the binding energies of low-lying yrast states in both odd and even $^{102-132}\text{Sn}$ -isotopes. Due to the lack of existing experimental data and the near degeneracy in energy of the relevant $0g_{7/2}$ and $1d_{5/2}$ single-particle orbits, a microscopic shell-model description of the configurations of nuclei in the trans-tin region was a challenging task. As described from the simple perspective of generalized seniority scheme, the excitation energies of the first 2^+ states in tin isotopes between ^{102}Sn and ^{132}Sn possess an almost constant value. The realistic shell-model description of these nuclei requires knowledge of the effective interaction between the valence nucleons that govern the dynamics. These realistic effective interactions obtained from nucleon-nucleon potentials

*Corresponding author (E-mail: sunilduttamu@gmail.com)

provide a microscopic foundation to shell-model calculations.

The structure and decay properties of light nuclei between helium-4 and Sn-100 as well as heavy nuclei around shell closures have been successfully explained with the shell-model calculations with empirical relations¹. The key to these calculations is the proper description of the monopole channel of the effective interaction^{6, 9}. This monopole channel determines the bulk properties of the effective interaction and governs the evolution of the effective single-particle energies as a function of valence neutron and proton numbers. Its contribution becomes much more important with increasing valence nucleon numbers N as the monopole interaction is proportional to $N(N-1)/2$.

Chong and Xu refined the unknown single-particle energies of the orbitals $1d_{3/2}$, $2s_{1/2}$, and $0h_{11/2}$ and the monopole interactions by fitting to experimental binding energies. They fitted the data for a total number of 157 states in ¹⁰²⁻¹³²Sn isotopes. The binding energies of these states were reproduced within an average deviation of about 120 keV. Which we have used in our calculations as an input to the many-fermion configuration-interaction shell-model code BIGSTICK^{10,11}. This code can calculate the energy spectra and occupation-space wave functions as well as the particle occupations, expectation values of operators, and static and transition densities and strengths. We can also use this code to determine the strength functions via Lanczos trick etc.

BIGSTICK gives us choice of Lanczos algorithm to quickly calculate the matrix elements as well as allows access to much larger spaces. Even though the basis dimensions have been discussed much in configuration interactions codes, nevertheless, the real gauge of the computational expenditure is the number of nonzero matrix elements. This number can be changed by using different truncations and therefore different densities.

In large-scale shell-model calculations, one sets up the model space and configurations that span the space for each J^π value. The basis configurations are denoted by $|(j_{p1}j_{p2} \dots)^{n_p} J_p, (j_{n1}j_{n2} \dots)^{n_n} J_n; JM\rangle$, meaning that one constructs the proton n_p particle state J_p and multiplies it by the neutron n_n particle state J_n , coupling both to total spin J . The basis has $n(J)$ basis configurations. Starting from the single-particle energies $\epsilon_{j_{p_i}}$, $\epsilon_{j_{n_i}}$ and the two-body matrix elements for identical and non-identical nucleons, one

builds up the energy matrix $[H_{ij}]$ and diagonalises the $n(J) \times n(J)$ energy matrix. Thus one obtains the $n(J)$ energy eigenvalues and $n(J)$ corresponding eigenfunctions. With the wavefunctions $\Psi_i(j_i^{\pi_i})$ and $\Psi_f(j_f^{\pi_f})$ we calculate the physical observables that we compare with the data and so improve iteratively upon the procedure.

In the present work, the one-body densities were calculated using BIGSTICK code whereas these calculated densities were used as in input to well established Oxbash code 'DENS'^{13,14} to determine the transition probabilities. Dens program calculates the radial wavefunctions for a given nucleus with an oscillator, Woods-Saxon or Skyrme Hartree-Fock potentials and reads the '*.obd' file with given single-particle transition probabilities from oxbash to calculate B(EL), B(ML) and B(GT) values.

2 Calculation for Sn-isotopes

In our calculations, we have defined five single-particle states $0g_{7/2}$, $1d_{5/2}$, $1d_{3/2}$, $2s_{1/2}$ & $0h_{11/2}$. The protons and neutrons were activated independently in all the orbits for all the Sn-isotopes except 114,116 and 118 Sn-isotopes. As for these mid-shell nuclei, huge inequality between protons and neutrons Slater determinants was observed, the protons were activated mainly in $0g_{7/2}$ and $1d_{5/2}$, whereas the neutrons were activated in $1d_{3/2}$, $2s_{1/2}$ & $0h_{11/2}$ orbits. After defining the model space the interaction matrix elements are needed by the BIGSTICK which can be defined in the one, two or possibly three-body space. The '*.int' file contained the single-particle energies (SPEs) and the monopole optimized two-body matrix elements (TBMEs). The default interaction file format for two-body interaction is derived from OXBASH/NuShell which can be in isospin-conserving formalism or explicit proton-neutron format.

For up to 12 neutrons as particles or holes the size of basis dimensions was moderate and therefore the standard procedure of diagonalization named as Lanczos with default convergence (choice 'ld' in BIGSTICK) was used. We kept 10 states to be printed with 300 iterations for Lanczos to run. These two factors affect the internal storage of all Lanczos vectors which are saved in the RAM of the computer and therefore have high limitations. The criterion for the convergence is that the energy value must be less than 0.0010 MeV. The condition of convergence is given as:

$$\delta_{\text{conv}} = \frac{\sum_{i=1}^{N_{\text{keep}} + 10} |E_i^{\text{new}} - E_i^{\text{old}}|}{\sqrt{N_{\text{keep}} + 10}}$$

Truncation was used for the mid-shell nuclei 114,116&118Sn as the BIGSTICK was not able to compute the excitation energies for the full valence space. The reduced one-body density matrices are given as:

$$\rho_K^f(ab) \equiv \frac{1}{\sqrt{(2K+1)}} \langle \Psi_f || \hat{c}_a^\dagger \otimes \hat{c}_b || \Psi_i \rangle$$

The reduced matrix element can be deduced as the sum of products of the density matrix elements and the reduced matrix elements between single-particle states, as given below:

$$\langle \Psi_f || \hat{O}_K || \Psi_i \rangle = \sum_{ab} \rho_K^f(ab) \langle a || \hat{O}_K || b \rangle$$

where $\langle a || \hat{O}_K || b \rangle$ are matrix elements between single-particle states, while the density matrices are matrix elements between many-body states. With these single-particle matrix elements, we can compute the transition matrix elements for any many-body matrix elements for specific operators like E2 and M1. However, we determined only the E2 matrix elements for 2→0 transition for all the studied nuclei.

Since ¹⁰⁰Sn and ¹³²Sn correspond to fully unfilled and filled shells, and hence, no nucleons were available in the valence space for the interaction to give rise to different states. Large unbalance between proton and neutron Slater determinants (SDs) for mid-shell nuclei is also not feasible with the code. Therefore, space was optimized for the best possible truncation for these isotopes. Weight was given to the neutrons in 1d_{3/2}, 2s_{1/2}, and 0h_{11/2} orbitals with a maximum truncation of 6,0,6 that correspond to total, proton, and neutron weights with good J-value./m-value.

As shown in Fig. 1, the calculated excitation energies up to state 10⁺ matches nicely with the experimental values. A maximum deviation of 270 keV for 2⁺ state was observed for ¹⁰²Sn, nevertheless, the average deviation was observed to nearly 100 keV. Further, in Fig. 2 we have plotted the E4/E2 ratio concerning the mass number of studied isotopes which show reasonably good agreement with the experimental data. We observed a maximum of 11% deviation for ¹⁰²Sn, however, for the rest of the isotopes, this discrepancy was observed to be less than 7%.

Till date, only a few states have been assigned experimentally in ¹⁰²Sn nucleus. In Fig. 3 we have presented a low-level energy scheme for ¹⁰²Sn nucleus calculated with BIGSTICK, which shows reasonably good agreement with the experimental levels. It is

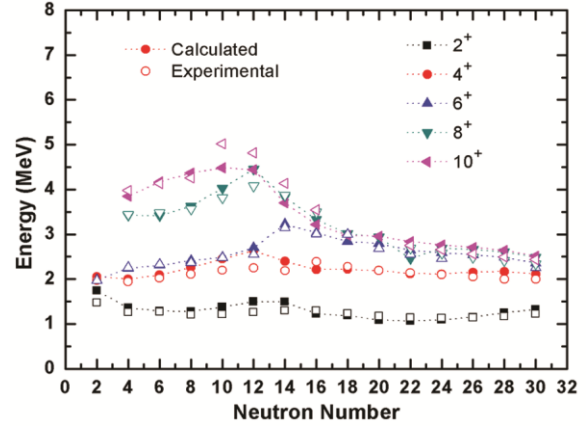


Fig. 1 – Experimental and calculated excitation energies of the low-lying positive parity yrast states in ¹⁰²⁻¹³⁰Sn-isotopes.

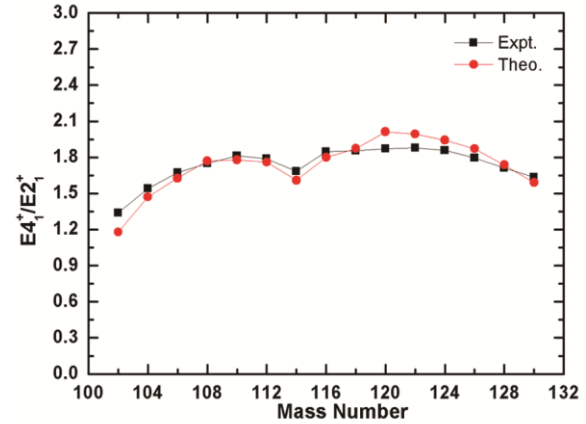


Fig. 2 – The variation of E4/E2 ratio in ¹⁰²⁻¹³⁰Sn isotopes.

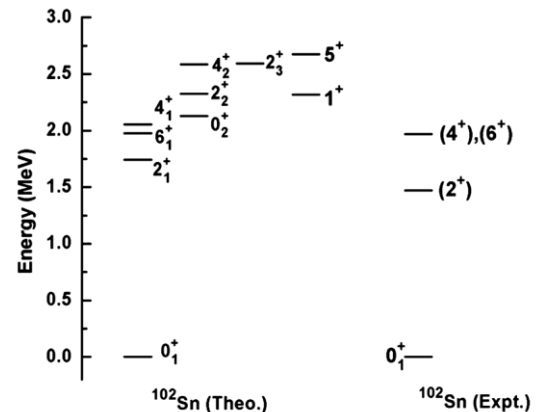


Fig. 3 – Low-level energy scheme for first 10 excited states in ¹⁰²Sn nucleus with available experimental levels¹³.

worth to mention that in the BIGSTICK calculations, we have considered only the positive parity states.

To calculate the transition probabilities the standard sample input for the ‘dens’ program was used. Dens is a nuclear density and electromagnetic form factor program which is a part of Oxbash package developed by B.A. Brown^{13,14}. We used ¹⁰⁰Sn as a core with valence space up to 1h_{11/2} orbital corresponding to shell-closure at 82. One-body transition densities calculated from BIGSTICK code were used as an input to the dens. BIGSTICK has a few choices to generate density matrices. We used the option to compute one-body densities from the previous run, which is given as ‘dx’ in the menu. For the good isospin in the interaction file, the one-body density matrices will be coupled to good isospin. But if the interaction file breaks the isospin, the density matrices will be taken in proton-neutron format. Since there are no valence protons, the BE2 values were not affected by the proton effective charge, therefore, in Fig. 4, we have only presented the values for different neutron effective charges. The BE2 values are found to underestimate the experimental BE2s for proton-rich isotopes whereas matches with reasonably good agreement for above mid-shell isotopes (118-130) for neutron effective charge equal to 0.9e.

3 Calculation for Ba-isotopes

The low-level energy spectra for the even-A stable Ba-isotopes (106, 108, 110, 112, 138, 136, 134 and 132) were calculated using the same interactions as used for Sn-calculations in the same gds_{h11/2} shell and have been presented in Figs 5-8.

As we know, Barium has atomic number 56 i.e. 6 more protons to closed-shell number 50, whereas the

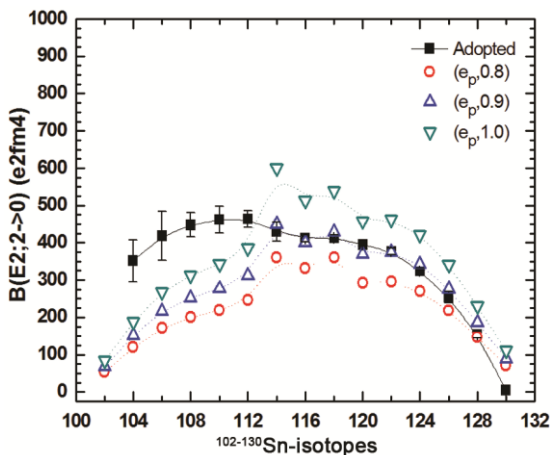


Fig. 4 – The calculated and adopted $B(E2; 2 \rightarrow 0)$ values (in e^2fm^4) for ¹⁰²⁻¹³⁰Sn-isotopes.

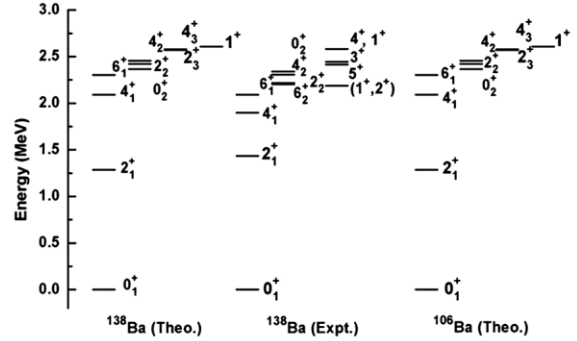


Fig. 5 – Low-level energy scheme for first 10 excited states in ¹³⁸Ba & ¹⁰⁶Ba nuclei with available experimental levels¹³.

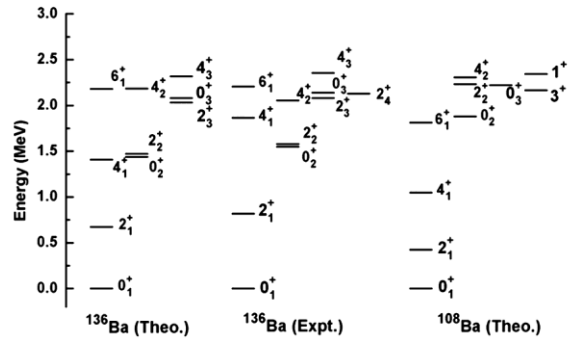


Fig. 6 – Low-level energy scheme for first 10 excited states in ¹³⁶Ba & ¹⁰⁸Ba nuclei with available experimental levels¹³.

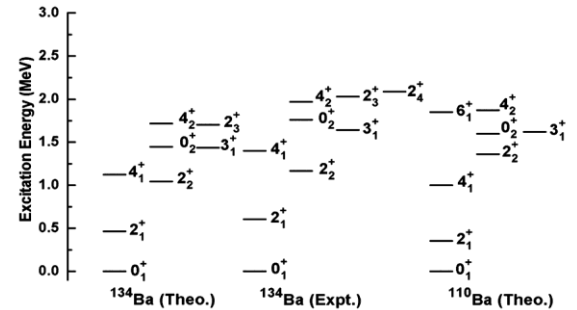


Fig. 7 – Low-level energy scheme for first 10 excited states in ¹³⁴Ba & ¹¹⁰Ba nuclei with available experimental levels¹³.

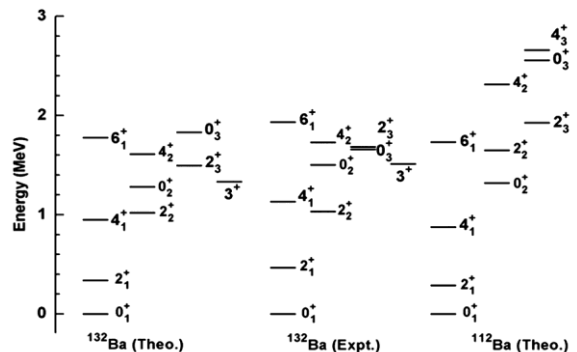


Fig. 8 – Low-level energy scheme for first 10 excited states in ¹³²Ba & ¹¹²Ba nuclei with available experimental levels¹³.

studied nuclei have 0, 2, 4 & 6 neutrons as particles and/or holes to closed shells 50 and/or 82. The barium has 130, 132, 134, 136 & 138 as the stable isotopes which are on the neutron-rich side and are well studied for their low-level energy spectrum. Nevertheless, there is no experimental data available for the proton-rich isotopes 106, 108, 110 and 112Ba which have also been studied in the present study. We have calculated the low-level energy scheme for these proton-rich barium isotopes and have been compared with the corresponding barium isotope with the same number of neutron holes as valence particles.

The partially calculated level schemes of $^{112,132}\text{Ba}$, which are a system with 6 protons being coupled to 6 neutron particles or neutron holes, have been shown in Fig. 8. These isotopes are the largest systems treated in the full/non-truncated shell-model space calculations. It is clear from the figure that the calculations reproduce the experimental spectrum of ^{132}Ba fairly well. In spite of the fact that for ^{112}Ba the spectrum is expected to be highly influenced by the strong proton-neutron interaction, the calculated spectra for ^{112}Ba and ^{132}Ba are somewhat close to each other.

The calculated and adopted excitation energies for $2^+ \rightarrow 0^+$ transition of stable $^{132-138}\text{Ba}$ isotopes have been shown in Fig. 9. The calculated transition probabilities with bare effective charges of $e_p, e_n = 0.5e, 0.5e$ shows close agreement with the experimental data and have been presented in Fig. 10.

4 Summary and Conclusions

In this chapter, we have used the BIGSTICK code to study the low-level excitation energies of even-A Sn and Ba-isotopes. A globally optimized effective interaction for $sdgh^{11/2}$ shell was used in the calculations. The low-level excitation energies for the even-A tin isotopes are found to be in good agreement with the NNDC data. Low-level energy spectrum for less studied ^{102}Sn nucleus have also been computed and presented. E4/E2 ratio systematic matches nicely with the experimental data for the isotopes from $^{102-130}\text{Sn}$. An overall good agreement with the calculated and experimentally determined values was observed. As discussed in reference¹⁴, the Pauli blocking may be responsible for the asymmetric electric quadrupole (E2) transition shape in Sn isotopes. As there were no valence protons, the BE2 values were not affected by

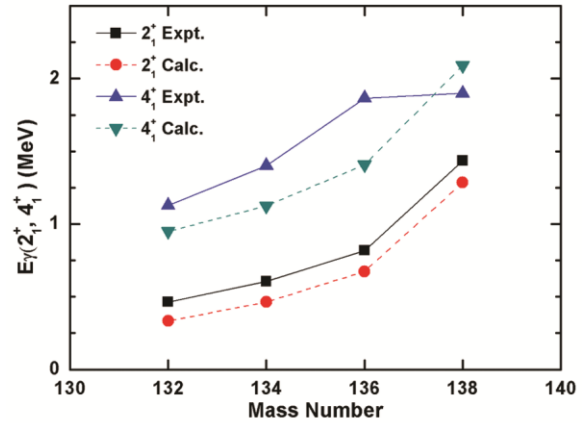


Fig. 9 – The variation of calculated and experimental excitation energies of first 2^+ & 4^+ states in $^{132-138}\text{Ba}$ isotopes.

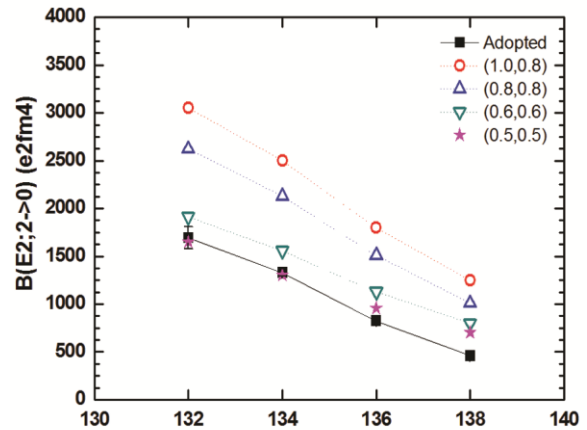


Fig. 10 – The calculated and adopted $B(E2; 2 \rightarrow 0)$ values (in $e^2\text{fm}^4$) for $^{132-138}\text{Ba}$ -isotopes.

the proton effective charge whereas a good agreement for neutron effective charge of $0.9e$ was observed. The code also reproduces well the low-level energies in the barium isotopes. For the studied isotopes, the energy spectrum for same number of neutron particles and holes have been compared, which shows different level schemes for the two isotopes. The calculated excitation energies for the stable isotopes show good agreement with the experimentally observed level-schemes. A good agreement for proton and neutron effective charges ($e_p, e_n = 0.5e, 0.5e$) was observed for the $B(E2; 2 \rightarrow 0)$ values in the studied Ba-isotopes.

Acknowledgement

The authors S.D. and C.Q. are thankful to KTH Royal Institute of Technology, Stockholm, Sweden for providing the financial support through Project No. 47591 to carry out the necessary facilities for pursuing the research work.

References

- 1 Caurier E, Martínez-Pinedo G, Nowacki F, Poves A & Zuker A P, *Rev Mod Phys*, 77 (2005) 427.
- 2 Brown B A, *Prog Part Nucl Phys*, 47 (2001) 517.
- 3 Parlett B N, *The symmetric eigenvalue problem*, SIAM, 7 (1980).
- 4 Press W H, Teukolsky S A, Vetterling W T, Flannery B P & Metcalf M, *Numerical recipes in fortran*, Cambridge University Press, 1992.
- 5 Whitehead R R, Watt A, Cole B J & Morrison I, *Adv Nucl Phys*, 9 (1977) 123.
- 6 Chong Qi & Xu Z X, *Phys Rev C*, 86 (2012) 044323.
- 7 Chong Qi, *J Phys G: Nucl Part Phys*, 44 (2017) 04.
- 8 Chong Qi, *Eur Phys J W C*, 175 (2018) 02015.
- 9 Bansal R K & French J B, *Phys Lett*, 11 (1964) 145.
- 10 Johnson C W, Ormand W E & Krastev P G, *Com Phys Commun*, 184 (2013) 2761.
- 11 Johnson C W, Ormand W E, McElvain & Shan Hongzhang, UCRL number LLNL-SM739926, arXiv: 1801.08432.
- 12 Brown B A, MSU-NSCL report number 1289.
- 13 www.nndc.bnl.gov/ensdf/
- 14 Back T, Qi C, Cederwall B, Liotta R, Moradi F G, Johnson A, Wyss R & Wadsworth R, *Phys Rev C*, 87 (2013) 031306(R).